

Supporting Information

Fluorine-Doped BP 2000: Highly Efficient Metal-Free Electrocatalysts for Acidic Oxygen Reduction Reaction with Superlow H₂O₂ Yield

Xiujuan Sun^{a,b,c}, Ping Song^{a,b}, Tao Chen^{a,b,c}, Jing Liu^{a,b} and Weilin Xu^{a,b,*}

^a State Key Laboratory of Electroanalytical Chemistry, Changchun Institute of Applied Chemistry, Chinese Academy of Science, 5625 Renmin Street, Changchun 130022, P.R. China.

^b Jilin Province Key Laboratory of Low Carbon Chemical Power, Changchun Institute of Applied Chemistry, Chinese Academy of Science, 5625 Renmin Street, Changchun 130022, P.R. China.

^c Graduate University of Chinese Academy of Science, Beijing, 100049, China.

1. Experimental Methods

The carbon black BP2000 was purchased from Asian-Pacific Specialty Chemicals Kuala Lumpur, Vulcan XC-72 and Pt/C (20 wt.% & 60 wt.%) were purchased from E-TEK Com. Ammonium fluoride (NH₄F) was purchased from Beijing Chemical Works, China, Potassium hydroxide (KOH) was purchased from Beijing Chemical Works, and Nafion solution (5 wt %) were obtained from Sigma-Aldrich. All the chemicals were used as delivered without further treatment. Ultrapure water with the specific resistance of 18.23 MΩ·cm was obtained by reversed osmosis followed by ion-exchange and filtration.

Fluorine doped BP 2000 catalysts were synthesized by directly annealing the mixture of Black Pearls 2000 (BP) and ammonium fluoride (NH₄F). The anneal treatment was carried out in a tube furnace with high argon as protective ambient. Detailed procedure is as follows: A given amount of NH₄F and BP 2000 were firstly dispersed in 10 ml H₂O. The mixture was sonicated for about 2 h and then stirred overnight. The resulting suspension was dried under vacuum at 40°C and then

pyrolyzed at 1000°C for 1h under argon atmosphere with flow rate of 80 mL/min.

After that, the sample was cooled down to room temperature and collected from the quartz tube. For comparison, the BP 2000 without F doping was treated in a similar way and denoted as BP 2000. In this work, the original mass ratio of NH₄F and BP 2000 are 10, 18 and 20. As a result, the F doped samples are denoted as BP-10F, BP-18F and BP-20F, respectively.

For F-doped Vulcan XC-72, all of the processes are the same as that F doped BP 2000, except that Vulcan XC-72 was used instead of BP 2000. The obtained products were denoted as Vulcan XC-18F.

2. Characterization

The transmission electron microscopy (TEM) images were obtained on a JEM-2100F microscopy with an accelerating voltage of 200 kV. Photoelectron spectroscopic (XPS) measurements were performed on a AXIS Ultra DLD (Kratos company) using a monochromic Al X-ray source. The Brunauer-Emmett-Teller (BET) surface areas obtained from 77 K N₂ sorption isotherms using ASAP 2020 instrument. The Raman spectroscopy was performed using a with a laser source of 633 nm.

3. Electrochemical Measurements

The activity for the oxygen reduction reaction (ORR) was evaluated by voltamperometry by the fluorine-doped BP 2000 (BP-F) as electrodes. A glassy carbon rotating disk electrode (4 mm in diameter) was used after polished with a 0.3 and 0.05 μ m alumina slurry and rinsed with water and ethanol several times.

Fabrication of the working electrodes was done by mixing 5 mg of BP 2000, BP-F catalysts, 50.0 μ L of a 5 wt % Nafion solution in alcohol, and 950.0 μ L of ethanol under ultra-sonication. A 10- μ L aliquot of the ink was dropped on the surface of the glassy carbon rotating disk electrode, yielding an approximate catalyst loading of 0.05 mg. For comparison, a commercially available platinum/carbon catalyst (20 wt % Pt on carbon black from E-TEK) ink was obtained by mixing 1 mg catalyst, 50 μ L of a 5 wt % Nafion solution in alcohol, 950 μ L of ethanol. Then, a 15- μ L aliquot of the platinum ink was dropped on the glassy carbon rotating disk electrode, yielding an approximate loading of 0.015 mg or 24 μ g Pt cm⁻².

The electrochemical performance was conducted in 0.5 M H₂SO₄ solution; the counter and the reference electrodes were a platinum wire and a SCE electrode, respectively. The potential of the electrode was controlled by a CHI 750E system (CH Instrument Co., USA). Rotating ring disk electrode (RRDE) tests were conducted on RRDE-3A apparatus (ALS company, Japan) with the Glassy Carbon disk and Pt ring electrode (the diameter is 4 mm for disk). Cyclic voltammetry (CVs) were performed from 1.0 to -0.2 V at 50 mV s⁻¹ after purging the electrolyte with O₂ or N₂ gas for 30 min. Voltamperometry measurements were performed by using the rotating ring-disk electrode (RRDE) at different rotating speeds from 225 to 1600 rpm in an O₂-saturated electrolyte from 1.0 to -0.2 V (vs. SCE) at a sweep rate of 5 mV/s in O₂ saturated 0.5 M H₂SO₄ solution.

For the calculation of yields of H₂O₂ on different catalysts, based on both ring and disk currents from RRDE, the percentage of HO₂⁻ generated from ORR and the

electron transfer number (N) were estimated by the following equations:

$$(1) HO_2^- \% = 200 \times \frac{i_R/0.37}{i_D + i_R/0.37}$$

$$(2) N = 4 \times \frac{i_D}{i_D + i_R/0.37}$$

Where i_D is the disk current density, i_R is the ring current density and 0.37 is the current collection efficiency of the Pt ring disk from the reduction of $K_3Fe[CN]_6$.

All potentials were conducted to the reversible hydrogen electrode (RHE). The method of calibration of SCE and conversion to RHE is according to reference. In 0.5 M H_2SO_4 solution, $E(RHE) = E(SCE) + 0.295$ V.

All the current densities have already been normalized to the electrode surface area.

All potentials were conducted to the reversible hydrogen electrode (RHE).

4. The structure and morphology of BP-18F electrocatalysts

The structure and morphology of BP and BP-18F electrocatalysts were investigated by transmission electron microscopy (TEM) as shown in Fig. S1. Large amount of BP-18F (Fig. S1b) thin sheet packed together and the mesopore structures can be clearly seen compared with granulous morphology of BP (Fig. S1a). Figure s1c shows the typical N_2 adsorption-desorption curve of BP-18F, a type IV curve with a hysteresis loop ($P/P_0 > 0.4$), which means that the catalysts are mesoporous materials. The increase of BET surface area from $1217\text{m}^2/\text{g}$ to $1735\text{m}^2/\text{g}$ after F-doping probably could be attributed to the formation of thin sheet structure. This fact indicates the doped-F atoms probably could catalyze the surface restructuring of carbon at high temperature.

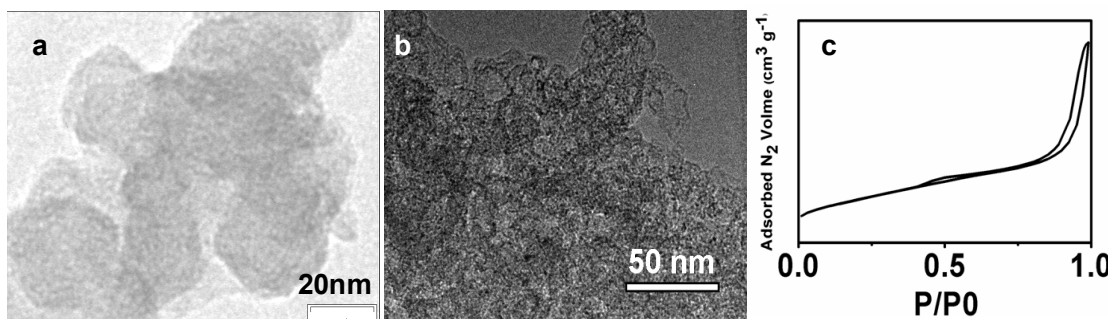


Fig.S1. TEM images of pure BP(a) and BP-18F (b), and (c) N₂ sorption curve for BP-18F catalysts.

5. The electrocatalytical performance for BP, BP-10F, BP-18F and BP-20F

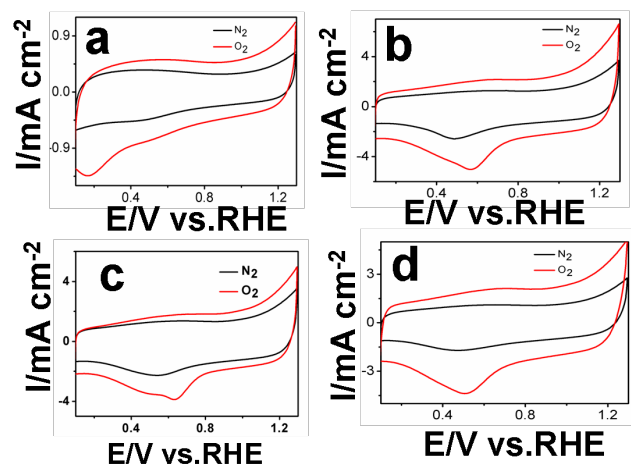


Fig.S2. CV results of BP (a), BP-10F (b), BP-18F (c) and BP-20F (d) catalysts in 0.5 M H₂SO₄ saturated with N₂ (black line) and O₂ (red line), respectively. Catalyst loading was 0.4 mg/cm⁻² for all samples.

Fig.S2 shows the CVs of BP and BP-F electrocatalysts in 0.5 M H₂SO₄ saturated with N₂ (black line) and O₂ (red line). Only a small O₂ reduction peak appeared at 0.19 V in O₂ saturated 0.5 M H₂SO₄, indicating very poor ORR electrocatalytical activity for BP. All of the F-doped BP catalysts exhibit O₂ reduction peaks that much more positive than BP, which indicated that the BP-F catalysts posses better ORR

activities than BP in 0.5 M H₂SO₄ solution. The reduction peak potentials for BP-10F, BP-18F and BP-20F catalysts are at 0.57 V, 0.63 V and 0.55 V, respectively. These results for the CVs demonstrated that the doping of F significantly enhanced the ORR of BP in 0.5 M H₂SO₄ solution.

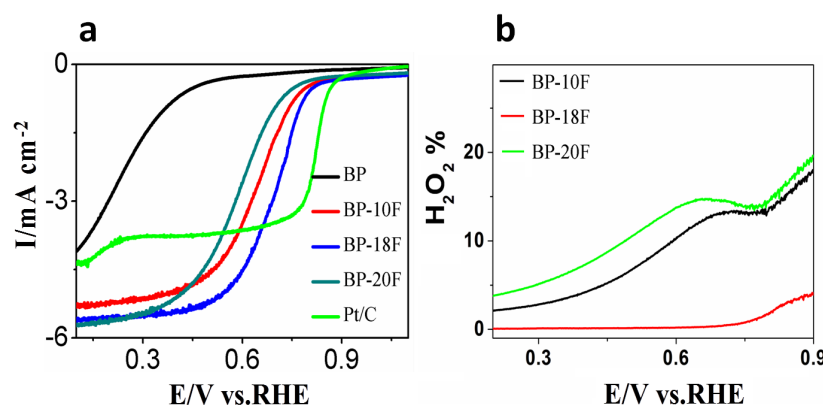


Fig.S3. (a)LSV results of BP, BP-10F, BP-18F, BP-20F and Pt/C catalysts in O₂-saturated 0.5 M H₂SO₄ with the scan rate of 5 mV/s and the rotation speed 1600 rpm.(b) H₂O₂ yield on different BP-F catalysts.

Fig.S3a shows the LSVs for BP, BP-10F, BP-18F, BP-20F and commercial Pt/C (E-TEK Company 20 wt %) in O₂ saturated 0.5 M H₂SO₄ when the scan rate is 5 mV/s and the rotation speed is 1600 rpm. As can be seen, the onset potentials for BP-F catalysts are 0.87 V, 0.90 V and 0.86 V for BP-10F, BP-18F and BP-20F, respectively, while for BP is 0.59 V. The pronounced elevated onset potentials of the BP-F catalysts compared to pure BP demonstrated that the doping of F improve the ORR activity of BP. **Fig.S3b** shows the H₂O₂ yields on different BP-F catalysts. From it we can see the H₂O₂ yield of catalyst depends on F-content in a volcano-shape. At an optimal F-content on carbon, the highest performance could be obtained.

5. The XPS spectrum of C 1s for BP-18F and BP

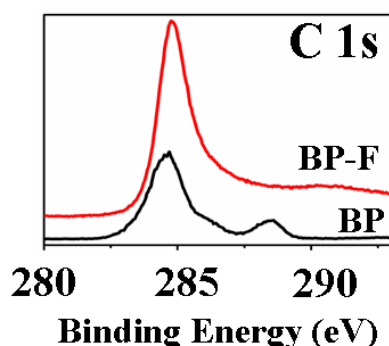


Fig.S4 Comparison of the high-resolution XPS spectrum of C 1s for BP-18F (red) and BP (black)

As can be seen, for pure BP, the binding energy at about 284.7 eV and 288.5 eV can be assigned to C=C and C=O respectively, no peaks for C-F is observed. After F doped into BP, an obvious peak at about 290.9 eV confirms the formation of semi-ionic C-F bond.

6. Density functional theory

To get more insight into the electrocatalytic activity of CB-F catalysts, quantum calculation has been done to study the O₂ adsorption with density functional theory (DFT) method with Gaussian 09.¹ In general, the active sites focus on the vacancy part, and more peripheral carbon atoms will play less prominent role in the active site. As well as the vacancy structure for CB, one pure CB model (including 65 atoms) with a vacancy effect has been constructed, which should be large enough to include the active sites.²⁻⁷ The oxygen groups on the edge of the models represent the oxygen types in CB. In addition, F is supposed to suspend over the surface of CB to form F-doped CB (CB-F) (in Table 1). The larger electronegativity for F atom can evoke

the C atoms adjacent to it with more positive charge, which are favorable to capture O₂. Then the distance between O₂ and CB-F is shorten to 2.661 Å comparing with that in pure CB, confirming the capture ability of O₂ for CB-F. As is known to us, the adsorption energy for O₂ is one of the most important indexes for ORR process. The larger the adsorption energy, the greater action in weakening O-O bond to form the following intermediate. After F-doping, the larger adsorption energy (-0.36 eV) between CB-F and O₂ than pure CB (-0.04 eV) demonstrates superiority for O₂ adsorption on CB-F, and the O-O bond has been extended to 1.254 Å comparing with 1.217 Å in pure CB. It is to say that there is nearly no interaction between pure CB and O₂ molecule. The effect of F in enhancing O₂ adsorption has also been investigated by natural bond orbital analysis (NBO). The natural population analysis (NPA) shows O₂ processes more negative charge (-0.31 e) in CB-F than that in pure BP (-0.02 e), i.e., the F-doping promotes the charge transfer from CB-F to O₂. The second-order perturbation energies ($E(2)$, $E(2)=q_iF_{ij}^2/(\epsilon_j-\epsilon_i)$), where F_{ij} is the off-diagonal element in the NBO Fock matrix, q_i is the donor orbital occupancy, and ϵ_i and ϵ_j are diagonal elements (orbital energies) with corresponding NBO orbital have been listed in Figure xx in the text to describe the much weak interaction between CB surface and O₂ molecule. Herein, BD, BD*, 3C* and LP represent 2-center bond, 2-center antibond, 3-center antibond and 1-center valence lone pair (n), respectively. According to the NBO analysis in the current paper, BD(2) and BD*(2) indicate π - and π^* -type orbitals. From Fig.S5, we can see there are only two small $\pi-\pi^*$ interactions between C-C bonding and O-O antibonding in the non-doped CB.

By contrast, the F-doping evokes more sets of overlaps between CB and O₂, leaving larger E(2) up to about 50 kJ/mol. One set is the interaction between 3C*-C1-C2-C3 and O-O, and the other is that between n-O and 3C*-C1-C2-C3. Herein, only two formations have been listed in Fig.S5 on behalf. In other words, the doping of F increases the interaction between CB-F surface and O₂ molecule, which enhances the activation of electron for carbon critical for the ORR.⁸ Based on the preceding analysis, the doping of F induces more positive charge on CB-F in favor of O₂ adsorption, and then enhances the interaction between O₂ and catalysts. Consequently, it increases the active electrons for carbon, thus indicating higher catalytic activity of CB-F for ORR.

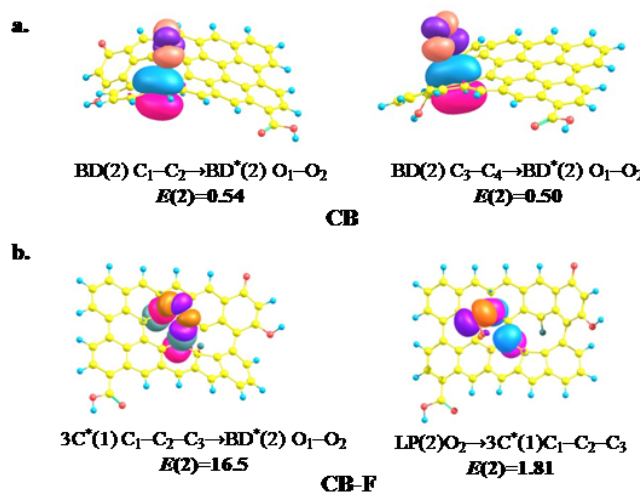


Fig.S5. The main NBO orbitals in non-doped CB (a) and CB-F (b) by NBO analysis (Units: kJ/mol).

7. The performance of Vulcan XC-72 carbon-based CB-F catalysts

The RDE measurements of F doped Vulcan XC-72 for ORR is shown in Fig. S6. The CVs of Vulcan XC-18F measured in N₂ and O₂ saturated 0.5 M H₂SO₄ solution was shown in Fig.S6a. An obvious peak at about 0.59 V vs. RHE indicated that

Vulcan XC-18F catalysts exhibit high ORR performance. The onset potential obtained from the LSV curves is about 0.87 V vs. RHE (Fig.S6b). As for the Vulcan-F catalysts, it can be seen the onset potential of the optimal one is close to that of the optimal BP-F, but the H₂O₂ yield is not as low as that on BP-18F (Fig.S6c), indicating the performance of catalyst largely depends on the carbon source.

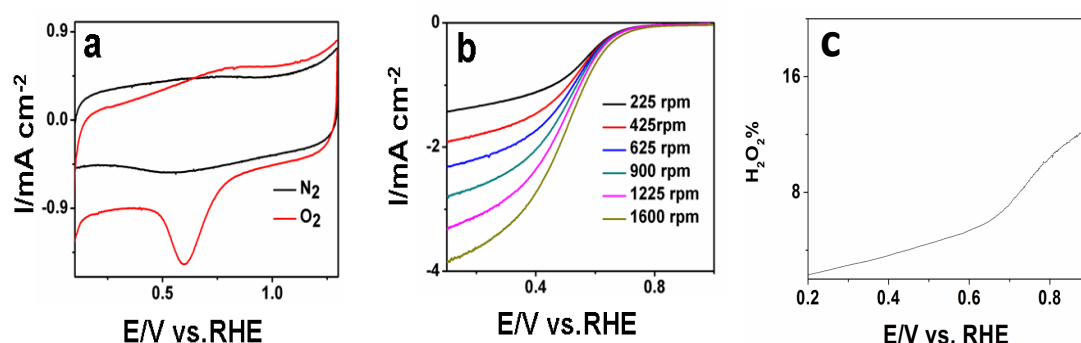


Fig.S6. CV (a) and LSV (b) curves for ORR on Vulcan XC-F in 0.5 M H₂SO₄. (c) The H₂O₂ yield on Vulcan XC-F.

1. M. Frisch, G. Trucks, H. Schlegel, G. Scuseria, M. Robb, J. Cheeseman, G. Scalmani, V. Barone, B. Mennucci and G. Petersson, Gaussian, Wallingford, 2010.
2. Y. Liang, Y. Li, H. Wang, J. Zhou, J. Wang, T. Regier and H. Dai, *Nat Mater*, 2011, **10**, 780-786.
3. K. Gong, F. Du, Z. Xia, M. Durstock and L. Dai, *Science*, 2009, **323**, 760-764.
4. V. R. Stamenkovic, B. Fowler, B. S. Mun, G. Wang, P. N. Ross, C. A. Lucas and N. M. Marković, *Science*, 2007, **315**, 493-497.
5. B. Fang, N. K. Chaudhari, M.-S. Kim, J. H. Kim and J.-S. Yu, *J. Am. Chem. Soc.*, 2009, **131**, 15330-15338.
6. C. Wang, H. Daimon and S. Sun, *Nano Letters*, 2009, **9**, 1493-1496.
7. M. K. Debe, *Nature*, 2012, **486**, 43-51.
8. L. Yang, S. Jiang, Y. Zhao, L. Zhu, S. Chen, X. Wang, Q. Wu, J. Ma, Y. Ma and Z. Hu, *Angew. Chem. Int. Ed. Engl*, 2011, **123**, 7270-7273.